IRJSE *Int. Res. J. of Science & Engineering,* 2017; Special Issue A1 : 123-127 SJIF Impact Factor 4.11
ISSN: 2322-0015 UGC Approved Journal No. 63628
RESEARCH ARTICLE **OPEN ACCESS**

Band Gap Energy of $Ni_{1-x}Cd_xY_yFe_{2-y}O_4$ by Sol-gel Method

Bhise RB[1] and Rathod SM[2]

[1]Department of Physics, B.J. College, Ale, Tal: Junnar, Dist: Pune, 412411, India,
[2]Nanomaterials and Laser Research Laboratory, Abasaheb Garware College, Pune, 411004, India
Email: bhiseramesh@gmail.com

Manuscript Details
Available online on http://www.irjse.in
ISSN: 2322-0015

Editor: Dr. Arvind Chavhan

Cite this article as:
Bhise RB and Rathod SM. Band Gap Energy of $Ni_{1-x}Cd_xY_yFe_{2-y}O_4$ by Sol-gel Method, *Int. Res. Journal of Science & Engineering,* December 2017; Special Issue A1 : 123-127.

ABSTRACT

Nanoparticles of Y^{3+} substituted $Ni_{1-x}Cd_xY_yFe_{2-y}O_4$ (where x = 0, 0.2, 0.4, 0.6 and y = 0, 0.075) were synthesized using sol-gel autocombustion method. The investigation of optical properties was carried out for the synthesized samples using Fourier transform infrared spectroscopy (FTIR) and Ultraviolet visible spectrophotometer (UV-Vis). XRD revealed that the structure of these nanoparticles is spinel with average grain size lies in the range between 12.5 to 34.8 nm. Lattice parameter was found to increases with Ni-Cd concentration and this may be due to the larger ionic radius of the Y^{3+} ion. The energy band gap was calculated using Tauc method for samples with different ratio and average band gap energy was found to be 1.6294 eV. The substitution was resulted in slight increase in the lattice constant and that sequentially may lead to the slightly increased in the energy gap.

Keywords: Autocombustion Method, Band Gap, Optical Property.

INTRODUCTION

Material technology associates the knowledge from the fields of physical science, chemical science, and Engineering. The wide applications of nanoparticles are in electronic, mechanical, optical, and magnetic devices, tissue engineering, magnetic storage systems and magnetic resonance imaging [1-2]. Material technology is new technique for processing manipulation and assembly using atoms, molecules or macromolecules for the

intelligent design of functional materials, components and systems with attractive qualities and functions [3-4]. Magnetic nanomaterials intensively studied as a recording media due to their superior physical properties. These properties make ferrites an ideal candidate for technical applications such as magnetic resonance imaging enhancement, catalysis, sensors and pigments [5]. Combined spinel ferrites have been studied intensively over the last few years due to their potential applications. Spinel ferrites have the chemical formula MFe_2O_4 in which M can be any divalent metal cations. In spinel ferrite, oxygen forms face centre cubic (FCC) lattice with divalent cations at tetrahedral (A) and/or octahedral (B) sites. Magnesium ferrite ($MgFe_2O_4$) has an inverse spinel structure with the preference of Mg^{2+} cations mainly on octahedral sites [6-9], while Zinc ferrite ($ZnFe_2O_4$) has normal spinel structure, in which Zn^{2+} cations mainly occupy tetrahedral sites [6-10]. The small scale size of the well-known spinel ferrites has opened up the door for intensive research to utilize their properties for biomedical applications [11-13]. Numerous methods were reported in literature showing the possibilities of producing particle size in the range of 2 - 100 nm [14-15]. In this work, $Ni_{1-x}Cd_xY_yFe_{2-y}O_4$ (where x = 0, 0.2, 0.4, 0.6 and y = 0, 0.075) were synthesized using co-precipitation methods. X-ray diffraction was used to investigate the structural and Ultraviolet visible spectrometer and Fourier Transform Infrared Spectroscopy were used to investigate the optical properties of crystallite nanoparticles.

METHODOLOGY

The Y^{3+} doped in Ni-Cd ferrite powders were synthesized by sol-gel autocombustion method at low temperatures for different compositions of $Ni_{1-x}Cd_xY_yFe_{2-y}O_4$ (where x = 0, 0.2, 0.4, 0.6 and y = 0, 0.075). The AR grade nitrate of Merck company (purity of 99%) are used in the experiments such as Yttrium nitrate ($Y(NO_3).6H_2O$), Nickel nitrate ($Ni(NO_3)\cdot 6H_2O$), Cadmium nitrate ($Cd(NO_3)\cdot 6H_2O$), Ferric nitrate ($Fe(NO_3)_3.9H_2O$). These nitrates and citric acid are using stoichiometric ratio proportion to obtain the final product and the citric acid ($C_6H_8O_7$) is used as a fuel in the ratio 1:3. The proportion of each reagent was defined according to its respective molar amounts [16]. All chemicals are dissolved in distilled water and were stirred till to obtain the homogeneous solution. To maintain pH equal to 7 by adding drop by drop ammonium hydroxide (NH_4OH) during the stirring process. This solution was stirred continuously with 80 °C for about 4-5 hours to obtain sol. After 4-5 hours, gel converts into ash and ash convert into powder. Finally get fine powder of $Ni_{1-x}Cd_xY_yFe_{2-y}O_4$ ferrite nanoparticles after auto combustion. The powder was sintered at 400 °C for 2 hours.

The structural characterization was done using XRD analysis. The X-ray diffractometer with Cu-Kα radiation of wavelength 1.5405 A^0 at 40 kV performed a scanning from 20 to 80 degree at a step size of 0.02 degree per second for each prepared sample and determined crystal structure, lattice parameter and crystallite size. The optical characteristics was studied using Fourier Transformation Infrared spectroscopy (FTIR) of Bruker 3000 Hyperion microscope with vertex 80 single point detector performing images resolution ranging between 7500 to 450 cm^{-1} and UV-Visible spectroscopy. Further investigations of the optical properties are under way to elucidate the effective role of inter particle interactions in these samples.

RESULTS AND DISCUSSION

3.1 Structural Studies:

XRD analysis: The resulting powder $Ni_{1-x}Cd_xY_yFe_{2-y}O_4$ (where x = 0, 0.2, 0.4, 0.6 and y = 0, 0.075) nanocrystals were characterized by XRD pattern. The XRD pattern of sintered Y^{3+} doped the nickel-magnesium-cadmium ferrite nano crystals as shown in figure-2. Obtained XRD pattern and crystalline phases were identified and it conformed the formation of a homogeneous well-defined spinal cubic structure with put any impurity. The broad peaks in the XRD pattern indicate a fine particle nature of the particles. The particle size was determined using Scherer's formula.

The average particle sizes of nanoparticles are given in Table-1. The particle size decreases as the

concentration of Y^{3+} increases. Lattice parameter obtained for prepared sample is ranging between 8.3399 to 8.3665 A^0 and average grain size ranging between 12.5 to 34.8 nm. The deviation in lattice parameter can be attributed to the cations rearrangement in the nano sized prepared ferrites. Value of lattice constant for Ni-Cd doped Yttrium ferrite shows the expansion of unit cell with rare earth doping when compared with pure Yttrium ferrite. This is expected due to substitution of large ionic radius of Y^{3+} ions (0.9 A^0) with small ionic radius Fe^{3+} ions (0.645 A^0). This result in Y^{3+} substituted ferrites to have higher thermal stability relative to Ni-Cd ferrite.

Table-1: The particle size of $Ni_{1-x}Cd_xY_yFe_{2-y}O_4$ by XRD

Composition	Average grain size (t) nm	Lattice constant (a) A°
$NiFe_2O_4$	**34.77**	**8.3399**
$Ni_{0.8}Cd_{0.2}Fe_2O_4$	**25.15**	**8.3455**
$Ni_{0.8}Cd_{0.2}Y_{0.075}Fe_{1.925}O_4$	**20.76**	**8.3591**
$Ni_{0.6}Cd_{0.4}Y_{0.075}Fe_{1.925}O_4$	**16.05**	**8.3635**
$Ni_{0.4}Cd_{0.6}Y_{0.075}Fe_{1.925}O_4$	**12.49**	**8.3665**

Table-2: The band gap energy of $Ni_{1-x}Cd_xY_yFe_{2-y}O_4$ byUV- Visible spectroscopy

Composition	Wavelength (nm)	Band gap energy (eV)	
		Tangent Method	Tauc Method
x=0.2, y=0	**751.25**	**1.6505**	**1.6382**
x=0.2, y=0.075	**762.1**	**1.6270**	**1.6603**
x=0.4, y=0.075	**770.9**	**1.6085**	**1.6789**
x=0.6, y=0.075	**760**	**1.6315**	**1.6774**
Average Value		**1.6294**	**1.6637**

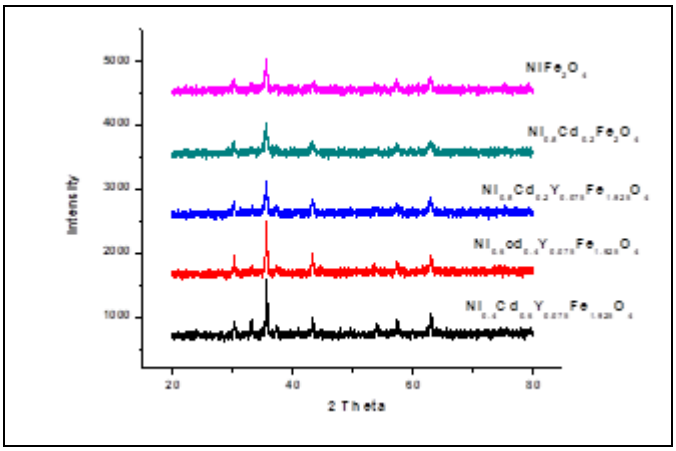

Figure 2: XRD pattern of $Ni_{1-x}Cd_xY_yFe_{2-y}O_4$

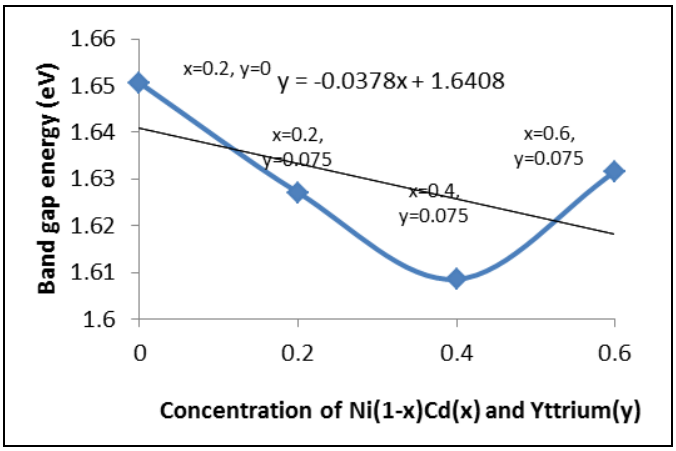

Figure 3: Variation of Band gap energy of $Ni_{1-x}Cd_xY_yFe_{2-y}O_4$ ferrite system with yttrium content(y)

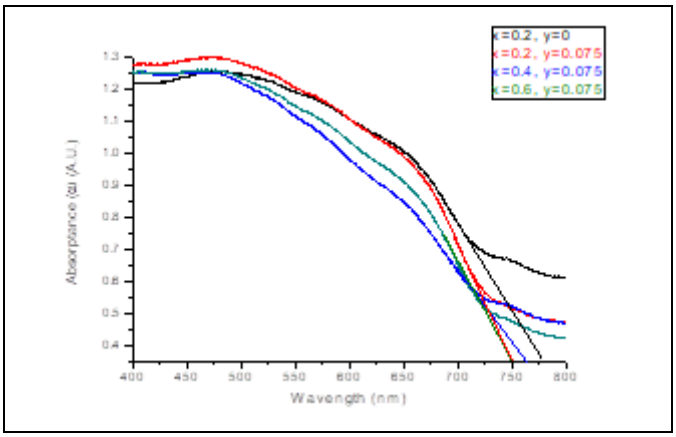

Figure 4: UV-Visible spectra of $Ni_{1-x}Cd_xY_yFe_{2-y}O_4$ nanoferites

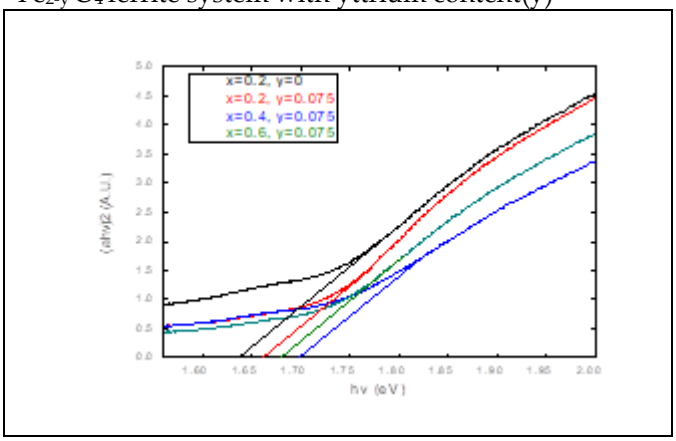

Figure 5: Band gap energy of $Ni_{1-x}Cd_xY_yFe_{2-y}O_4$ nanoferrites using Tauc method

3.2 Optical Studies:

a) UV Visible Analysis:

The figure-3 shows optical properties were studied from UV-Visible spectroscopy to calculate the band gap energy. In the absorption molecules of non-bonding electrons can absorb the energy in the form of ultraviolet or visible light to excite this electron to higher or anti-bonding molecular orbit. The energy band gap was calculated for samples. Energy band gap was found to be 1.6505, 1.6270, 1.6085 and 1.6315 eV. The substitution was resulted in slight increase in the lattice constant and that sequentially may lead to the slightly decrease in the energy gap. The average Band gap of prepared sample is 1.6294 eV and wavelength absorb by 761.06 nm. It is in the range of semiconductor materials.

The energy band gap was also determined by Tauc method for samples. It is 1.6505, 1.6270, 1.6085 and 1.6315 eV. The substitution was resulted in slightly decrease in the energy gap and the average Band gap is 1.6294 eV. It is also in the range of semiconductor materials.

b) FTIR Analysis: In order to investigate the chemical functional groups on the synthesized $Ni_{1-x}Cd_xY_yFe_{2-y}O_4$, FTIR spectroscopy are performed. The FTIR spectra of the prepared $Ni_{0.6}Cd_{0.4}Y_{0.075}Fe_{1.925}O_4$ are shown in figure 6 to know the bonding characteristics of the materials. The peaks at 476.71 cm^{-1} and 559.97 cm^{-1} are the peaks of Fe-O bond in Y doped Ni-Cd ferrite and it is arises due to the lattice vibrations of the oxide ions against cations. The peak at 1383.62 cm^{-1} indicates the presence of O-H bond due to bending vibration. The broad peak at 3431.91 cm^{-1} gives presence of hydroxyl group in the material and indicates that the material absorbed moisture from atmosphere during analysis.

The intense absorption bond is observed at 559.97 cm^{-1} which shows the characteristic bond of spinel structure which may due to presence of Fe-O and Y-O bonds or crystalline nature of Y doped Ni-Cd ferrite. Hence, FTIR analysis supports the observation of XRD analysis and confirms the crystalline nature of ferrite. So, the peaks at 476.71 cm^{-1} and 1032.57 cm^{-1} confirms the presence of yttrium doped in Ni-Cd ferrite. Finally, the doping of Y^{3+} on Ni-Cd ferrite was confirmed by different pattern of the plots and the difference in relative position and intensity of the peaks appeared in the FTIR plots of the prepared samples.

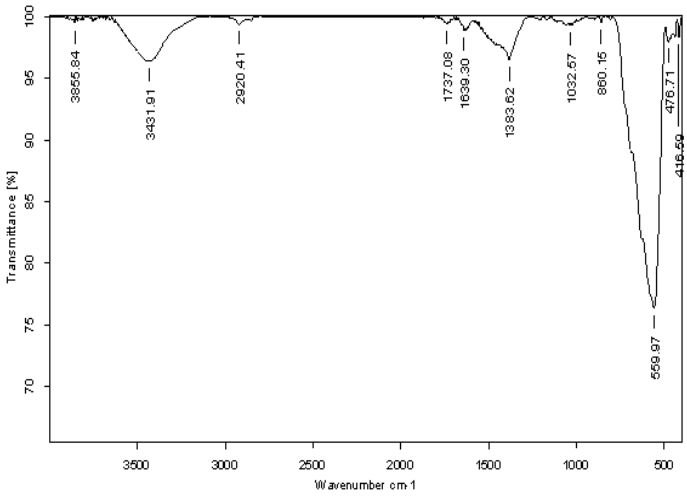

Figure 6: IR spectrum of $Ni_{0.6}Cd_{0.4}Y_{0.075}Fe_{1.925}O_4$ nanoferrites

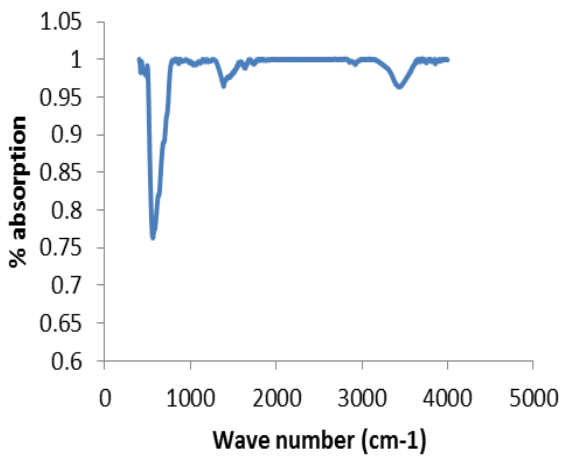

Figure 7: Absorption spectra of $Ni_{0.6}Cd_{0.4}Y_{0.075}Fe_{1.925}O_4$ ferrites

CONCLUSION

The $Ni_{1-x}Cd_xY_yFe_{2-y}O_4$ nanoferrites were synthesized using sol-gel autocombustion method. The increase in the Y^{3+} concentration gives the significant changes in the particle size and magnetic properties of the composition $Ni_{1-x}Cd_xY_yFe_{2-y}O_4$ (where x = 0, 0.2, 0.4, 0.6 and y = 0, 0.075). The prepared samples were characterized by XRD and shows that nanoparticles decrease with the increase in Y^{3+} content. The powders without Y^{3+} and Cd^{2+} presented small quantities of a second phase hematite (AFe_2O_4). The FTIR spectroscopy study shows two main metal oxygen bands in the range of 416.50 - 559.97 cm^{-1} confirming the formation of cubic spinel phase structure of Y^{3+} substitute in Ni-Cd ferrite. The synthesis of nanoparticles with crystalline size decreases and lattice constant increases as the concentration increases and is in the range of 12.5 to 34.8 nm for 400 ^oC. The UV-Visible analysis shows band gap energy increases with increase in Y^{3+} concentration and shows average band gap energy is 1.6294 eV at absorbed wavelength 549 nm. It is in the range of semiconductor materials. So that synthesized samples is in the nature of semiconductor materials.

REFERENCES

1. Flores-Acosta, M., Sotelo-Lerma, M., Arizpe-Chavez, H., Castillon-Barraza, F.F. and Ramirez-Bon, R.J. Excitonic Absorption of Spherical PbS Nanoparticles in Zeolite A. *Solid State Communications*. 2003;128:407-411.
2. Pulisova, P., Kovac, J., Voigtd, A. and Raschman, P. Structure and Magnetic Properties of Co and Ni Nano-Ferrites Prepared by a Two Step Direct Microemulsions Synthesis. *Journal of Magnetism and Magnetic Materials*. 2013;341: 93-99.
3. Lodhi, M.Y., et al.. New $Mg_{0.5}Co_xZn_{0.5-x}Fe_2O_4$ Nano-Ferrites: Structural Elucidation and Electromagnetic Behavior Evaluation. *Current Applied Physics*. 2014;14, 716-720.
4. Jan, L.S., Radiman, S., Siddig, M.A., Muniandy, S.V., Hamid, M.A. and Jamali, H.D. Preparation of Nanoparticles of Polystyrene and Polyaniline by γ-Irradiation in Lyotropic Liquid Crystal. *Colloids and Surfaces A: Physicochemical and Engineering Aspects*. 2004;251: 43-52.
5. Mathew DS and Juaug RS. An Overview of the Structure and Magnetism of Spinel Ferrite Nanoparticles and Their Synthesis in Micro Emulsions. *Chemi. Engi. Journal*. 2007; 129:51-65.
6. Rahman S, et al. Structural and Magnetic Properties of ZnMg-Ferrite Nanoparticles Prepared Using the Co-Precipitation Method. *Ceramics International*. 2013; 39: 5235-5239.
7. Pradeep A, Priyadharsini P and Chandrasekaran G. Sol-Gel Route of Synthesis of Nanoparticles of $MgFe_2O_4$ and XRD, FTIR and VSM Study. *Journal of Magnetism and Magnetic Materials*.2008;320:2774-2779.
8. Greenwood NN and Earnshaw A. Chemistry of the Elements; Pergamon Press Ltd., Oxford. 1984;279.
9. Ichiyanagi Y, Kubota M., Moritake S, Kanazawa Y, Yamada T and Uehashi T. Magnetic Properties of Mg-Ferrite Nanoparticles. *Journal of Magnetism and Magnetic Materials*. 2007; 310: 2378-2380.
10. Thummer KP, Chhantbar MC, Modi KB, Baldha GJ and Joshi HH Localized Canted Spin Behaviour in $Zn_xMg_{1.5-x}Mn_{0.5}Fe_2O_4$ Spinel Ferrite System. *Journal of Magnetism and Magnetic Materials*. 2004;280:23-30.
11. Kumara, C.S.S.R. and Mohammad F. Magnetic Nanomaterials for Hyperthermia-Based Therapy and Controlled Drug Delivery. *Advanced Drug Delivery Reviews*. 2011;63: 789-808.
12. Giri J, Pradhan P, Somani V, Chelawat H, Chhatre S, Banerjee R and Bahadur D. Synthesis and Characterizations of Water-Based Ferrofluids of Substituted Ferrites [$Fe_{1-x}B_xFe=O_4$, B=Mn, Co (x=0−1)] for Biomedical Applications. *Journal of Magnetism & Magnetic Materials*. 2008;320: 724-730.
13. Sharifi, I., Shokrollahi, H. and Amiri, S. Ferrite-Based Magnetic Nanofluids Used in Hyperthermia Applications. *Journal of Magnetism and Magnetic Materials*. 2012;324:903-915.
14. Chen, Y., Ruan, M., Jiang, Y.F., Cheng, S.G. and Li, W. The Synthesis and Thermal Effect of $CoFe_2O_4$ Nanoparticles. *Journal of Alloys and Compounds*. 2010;493:L36-L38.
15. Liu, Q., Sun, J.H., Long, H.R., Sun, X.Q., Zhong, X.J. and Xu, Z. Hydrothermal Synthesis of $CoFe_2O_4$ Nanoplatelets and Nanoparticles. *Materials Chemistry and Physics*. 2008;108:269-273.
16. Bhise RB and Rathod SM. June. Synthesis of Nanosized Y^{3+} Doped Ni-Mg-Cd Ferrite Powders and their Structural, Magnetic properties by Sol-gel Auto Combustion Method. *Res. J. Material Sci.*, 2016; 4(5), 1-4.